

## Ion-Exchange Reactions and Physical Properties of the Mica Analogue KNiAsO<sub>4</sub>

A. M. BUCKLEY, S. T. BRAMWELL, D. VISSER, AND P. DAY

*Inorganic Chemistry Laboratory, Oxford University, South Parks Road, Oxford OX1 3QR, England*

Received May 22, 1986; in revised form October 20, 1986

Exchange of  $RNH_3^+$  ( $R$  = saturated and unsaturated alkyl) and  $H_3O^+$  for  $K^+$  in the mica analogue  $KNiAsO_4$  has been investigated by chemical analysis, X-ray powder diffraction, infrared spectroscopy, and thermal analysis. For  $R = C_nH_{2n+1}$  with  $n = 1-10$ , the alkyl chains form ordered arrays between the inorganic layers and hydrogen bonding occurs between the  $-NH_3^+$  and the oxygen atoms of the arsenate groups. Under the same reaction conditions,  $RNH_3^+$  with one  $C=C$  or  $C\equiv C$  group or conjugated  $C=C-C\equiv C$  groups are not exchanged. Warming  $KNiAsO_4$  with 1 *M* HCl leads to partial replacement of  $K^+$  by  $H^+(H_2O)_y$ , but prolonged boiling with 1 *M* HCl removes all  $K^+$  to give  $Ni_3(AsO_4)_2 \cdot 6H_2O$ . On heating, the latter loses  $H_2O$  in two stages by a topotactic reaction, giving xanthosite,  $Ni_3(AsO_4)_2$ .  $KNiAsO_4$  and  $(C_{10}H_{21}NH_3)NiAsO_4$  become antiferromagnetically ordered below 20 K. The 10 K absorption spectrum of a single crystal of  $KNiAsO_4$  contains vibronic fine structure associated with the  ${}^1E(D) \leftarrow {}^1A_{2g}(F)$  ligand field transition, while the electronic origin line of the  ${}^3T_{1g}(P) \leftarrow {}^3A_{2g}(F)$  line at  $22,697 \text{ cm}^{-1}$  broadens and shifts to lower energy with increasing temperature. © 1987 Academic Press, Inc.

### 1. Introduction

In this paper the chemistry of a synthetic micallike compound, potassium nickel arsenate (1), will be discussed in terms of the ion exchange of its interlayer cations for organic and inorganic species.

In 1890, Lefevre described the preparation of arsenate compounds of the type  $M^I M^{II} AsO_4$  (2, 3) with  $M^I = K$  or Na and  $M^{II} = Ba, Sr, Ca, Pb, Mg, Mn, Zn, Cd, Ni,$  and Co. Ladwig and Ziemer (4) studied various physical properties of  $KNiAsO_4$  and suggested a trigonal unit cell ( $a_0 = 4.998$  and  $c_0 = 28.608 \text{ \AA}$ ) of space group  $R\bar{3}$ . A single-crystal X-ray study of  $NaNiAsO_4$  (5) confirmed that  $M^I NiAsO_4$  ( $M^I = K$  or Na)

crystallizes in a structure built up from tetrahedral-octahedral-tetrahedral three-sheet units, stacked along [001], giving a layer spacing of  $8.82 \text{ \AA}$  for  $NaNiAsO_4$  (5) and  $9.54 \text{ \AA}$  for  $KNiAsO_4$  (1, 4).

Each three-sheet unit is built up from a central two-dimensional infinite  $NiO_6$  octahedral sheet, where each  $NiO_6$  octahedron is connected with three other  $NiO_6$  octahedra. A network of six-membered rings built up from these octahedra is formed around unoccupied oxygen octahedra (Fig. 1a). The  $NiO_6$ -octahedral sheet is enclosed by two  $AsO_4$ -tetrahedral sheets. In these, three oxygen atoms of an empty octahedron form the basal plane for two  $AsO_4$  tetrahedra pointing up and down in the  $c$ -axis

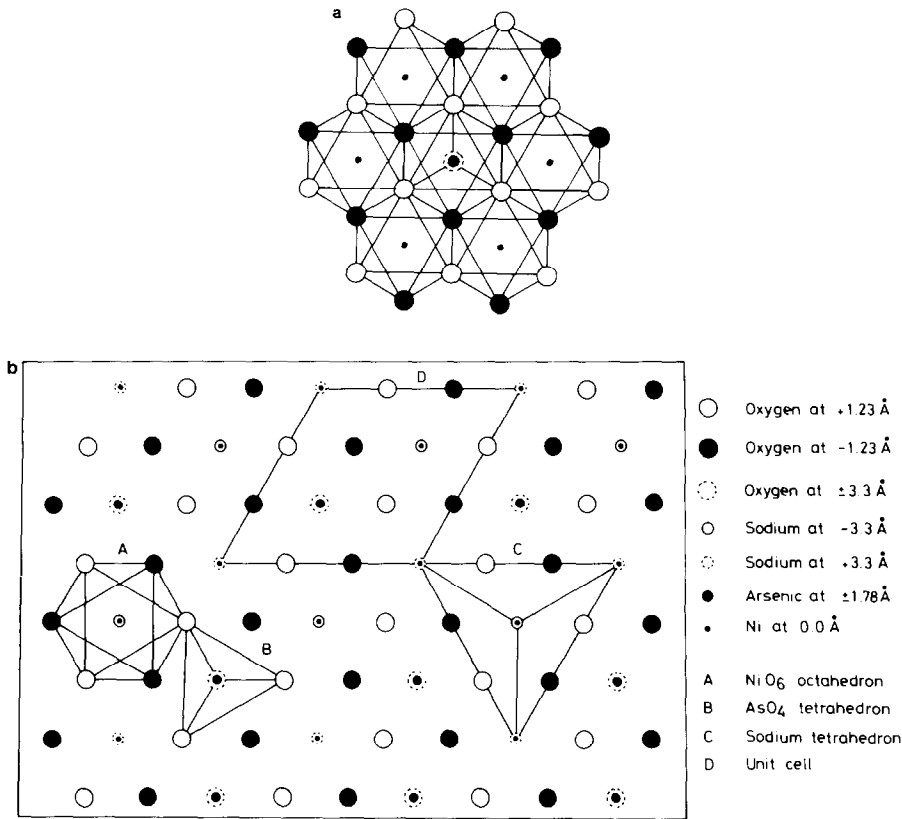


FIG. 1. (a) Packing of NiO<sub>6</sub> octahedra in NaNiAsO<sub>4</sub> and (b) projection of NiAsO<sub>4</sub> on the basal plane (25).

direction (Fig. 1b). The  $M^I$  atoms occupy isolated tetrahedra in the interlayers and have a (4 + 3) coordination.

Beneke and Lagaly found that KNiAsO<sub>4</sub> has a layer charge ( $74.3 \mu\text{C cm}^{-1}$ ) similar to that of brittle micas ( $69 \mu\text{C cm}^{-1}$ ) (1). Hence it was considered that KNiAsO<sub>4</sub> might be a possible model for studying ion-exchange reactions and the packing of alkylammonium ions. They prepared a series of compounds  $(\text{C}_n\text{H}_{2n+1}\text{NH}_3^+)_x\text{K}_{1-x}\text{NiAsO}_4$ .

In this paper we present further results on the ion-exchange chemistry of KNiAsO<sub>4</sub>, including an attempt to exchange unsaturated alkylammonium ions, as well as a study of the reaction with dilute aqueous acid. We have also investigated

the physical properties of KNiAsO<sub>4</sub> and its derivatives. Regnault *et al.* (6) showed that the structurally related  $\text{BaM}_2(\text{AsO}_4)_2$  ( $M = \text{Co}$  and  $\text{Ni}$ ) are examples of two-dimensional antiferromagnets, while layer perovskites with paramagnetic ions also exhibit two-dimensional magnetism when alkyl chains separate the layers (7). It is therefore of interest to discover the nature of the magnetism in KNiAsO<sub>4</sub> and its alkylammonium derivatives.

## 2. Experimental

### 2.1. Preparations

KNiAsO<sub>4</sub> was prepared by the method of Ladwig and Ziemer (4), who adapted the original method of Lefevre (2, 3).  $\text{Ni}(\text{NO}_3)_2$

(16.1 g) and  $\text{KH}_2\text{AsO}_4$  (19.9 g) were ground together and placed in a porcelain or platinum crucible. An excess of  $\text{KH}_2\text{AsO}_4$  is required (2:1,  $\text{KH}_2\text{AsO}_4:\text{Ni}(\text{NO}_3)_2$ ) so that the  $\text{KNiAsO}_4$  may crystallize out from molten  $\text{KH}_2\text{AsO}_4$  solution on cooling. The crucible was heated in a muffle furnace at  $1000^\circ\text{C}$  for approximately 3 hr, agitating occasionally in order to mix the reactants thoroughly. The melt was then cooled over 5 hr to  $400^\circ\text{C}$  and annealed at  $400^\circ\text{C}$  for 3 hr. The product was then left to cool to room temperature in the furnace. The resulting crystals were bright green mica-like plates. The solid was removed from the crucible and heated for about 5 min in boiling distilled water to dissolve the excess  $\text{KH}_2\text{AsO}_4$ . Ladwig and Ziemer's method (4), i.e., boiling for 5 hr in water, resulted in a form of  $\text{KNiAsO}_4$  which contained a much reduced proportion of potassium, as discussed in greater detail below. The suspension of  $\text{KNiAsO}_4$  was filtered and dried in air, giving 75% yield of  $\text{KNiAsO}_4$ .

Sorbyl amine (1-amino-2,4-hexadiene) for use in the ion-exchange reaction was prepared from sorbyl alcohol using the sequence described by Tieke and Wegner (8).

The ion-exchange experiments were carried out using the methods described for montmorillonites (9). About 1 g of  $\text{KNiAsO}_4$  was finely ground and aqueous solutions of  $\text{RNH}_3\text{Cl}$  were added to the  $\text{KNiAsO}_4$  powder with 0.2 ml of ethanol, then vigorously stirred under reflux at  $50^\circ\text{C}$ . After 24 hr the solution was filtered and the same volume of *n*-alkylammonium chloride solution added for another 24 hr. This was continued for up to 4 days. The samples were then freed from any alkylammonium chloride and alkylamine by washing with ethanol and ethanol:water, then dried in air. The crystals were considerably exfoliated with their color changing to a slightly lighter, more yellowish green. To study the hydration reaction  $10\text{ cm}^3$  of a 1 M acid (either HCl or  $\text{H}_2\text{SO}_4$ ) was added to about 5

g of the finely ground  $\text{KNiAsO}_4$ . The suspension was heated under reflux with stirring to about  $70^\circ\text{C}$  and kept at this temperature for 24 hr. The suspension was then filtered and the remaining solid returned to the flask with a new 10-ml portion of acid. Samples of the solid were removed at intervals during the reaction and characterized by chemical analysis and X-ray diffraction. After 72 hr the reaction was stopped and the solid residue was filtered and dried in air. Only about 0.2 g of a dull green solid remained, since the majority dissolved in the acid over the period of the reaction.

## 2.2. Characterization

Products were characterized by elemental analysis and by X-ray powder diffraction using a Philips diffractometer controlled by a Philips 1710 microprocessor and minicomputer. The temperature dependence of the powder X-ray diffraction pattern reaction of the  $\text{KNiAsO}_4$  and aqueous acid was also examined using a high-temperature Enraf Nonius Guinier-Simon Camera, in the Clarendon Laboratory, Oxford, at temperatures of 100, 280, 680, and  $800^\circ\text{C}$ .

Infrared spectra were recorded using a Perkin-Elmer 1710 Fourier transform infrared spectrometer, using samples in the form of KBr or CsI disks (inorganic derivatives) or hexachlorobutadiene mulls (organic derivatives).

Dehydration of the product of the reaction of dilute acid with  $\text{KNiAsO}_4$ , henceforth referred to as "the hydrated arsenate," was also studied by infrared spectroscopy. The spectrum of a KBr disk of the compound was first measured at room temperature. The disk was then heated in an oven at  $50^\circ\text{C}$  for 4 hr and the IR spectrum measured again. This was repeated in  $50^\circ\text{C}$  steps until there was no further change in the spectrum.

Thermogravimetric (TG) and differential thermal analysis (DTA) measurements

were performed on KNiAsO<sub>4</sub> and the hydrated arsenate at heating rates of 10°C/min and 4°C/min, respectively, using a Stanton Redcroft thermobalance. An additional TG experiment was carried out on hydrated KNiAsO<sub>4</sub> using a heating rate of 1°C/min up to 475°C, where the temperature was kept constant until the weight loss ended. Then the sample was heated up to 750°C at a rate of 10°C/min. The 750°C product was yellow/green and stable in air.

Magnetic susceptibilities were measured with an Oxford Instruments Faraday balance, consisting of a superconducting magnet combined with a Sartorius vacuum microbalance. The measurements were made at a field of 10 kOe and the susceptibility was corrected for the diamagnetic contribution.

Visible absorption spectra of KNiAsO<sub>4</sub> crystals were measured using a McPherson RS-10 spectrophotometer, which may be operated in single- or double-beam mode. The output is recorded via a digital voltmeter by a Research Machines 380Z microcomputer. With 10- $\mu$ m slits the resolution of the spectrometer is about 0.1 Å. The spectrometer is equipped with an Oxford Instruments CF100 continuous-flow helium cryostat and a Thor He cryostat incorporating a split-coil superconducting cyro-

magnet. Both cryostats have a Ge resistance thermometer and temperature controller.

### 3. Results

#### 3.1. Chemical Analysis

Analytical data for the RNH<sub>3</sub><sup>+</sup>-exchanged compounds are listed in Table I. The percentage ion-exchange values were calculated using the percentage of carbon found. Analyses calculated for complete ion exchange are given in parentheses. The extent of insertion of alkylammonium ions after 72 hr increases with the length of the alkyl chain, while the progress of the water exchange and acid attack is shown by the following analytical data:

	%K	Molar percentage
(0 hr)	16.57	100
(3 hr)	13.24	80.2
(48 hr)	4.47	27.1
(72 hr)	1.11	6.7

After 4 days when the K<sup>+</sup> content had reduced to 0.28%, the mole ratio of Ni:As had increased from 1:1 to 3:2.

#### 3.2. Powder X-Ray Diffraction

The diffraction profiles of the saturated alkylammonium nickel arsenates were

TABLE I  
ANALYTICAL DATA FOR (RNH<sub>3</sub><sup>+</sup>)<sub>x</sub>K<sub>(1-x)</sub>NiAsO<sub>4</sub> AFTER 72 HR EXCHANGE<sup>a</sup>

R	%N	%C	%H	%K	%Ni	x
K	—			15.08(16.51)	23.37(23.37)	0
CH <sub>3</sub>	1.91(6.09)	2.02(5.20)	1.27(2.6)	0.72(0)		0.39
C <sub>3</sub> H <sub>7</sub>	1.88(5.43)	5.69(14.00)	1.63(3.8)	5.21(0)	23.14(22.78)	0.41
C <sub>6</sub> H <sub>13</sub>	3.03(4.67)	15.94(24.03)	3.49(5.34)	0.34(0)	19.81(19.59)	0.66
C <sub>8</sub> H <sub>17</sub>	3.27(4.27)	22.94(29.30)	5.18(6.11)	0.76(0)	17.47(17.92)	0.78
C <sub>10</sub> H <sub>21</sub>	3.18(3.93)	27.93(33.75)	5.7(6.75)	0.73(0)	15.95(16.51)	0.83
C <sub>3</sub> H <sub>5</sub>	0.13(5.47)	0.57(14.08)	0	12.63(0)	23.04(22.95)	0.04
C <sub>6</sub> H <sub>9</sub>	1.78(4.74)	9.16(24.36)	1.29(4.06)	6.36(0)	22.83(19.86)	0.38
C <sub>3</sub> H <sub>3</sub>	1.44(5.52)	2.25(14.20)	Could not detect	9.59(0)	22.44(23.15)	0.16

<sup>a</sup> C<sub>3</sub>H<sub>5</sub> = CH<sub>2</sub>=CH·CH<sub>2</sub>; C<sub>6</sub>H<sub>9</sub> = CH<sub>3</sub>·CH=CH·CH=CH·CH<sub>2</sub>; C<sub>3</sub>H<sub>3</sub> = CH≡C·CH<sub>2</sub>.

TABLE II  
UNIT CELL PARAMETERS OF  $\text{KNiAsO}_4$  AND  
 $\text{K}_x(\text{RNH}_3)_{(1-x)}\text{NiAsO}_4$

R	This work		Ref. (1)	
	a (Å)	c (Å)	a (Å)	c (Å)
K	4.98	28.74	4.99	28.61
$\text{CH}_3\text{NH}_3$	4.98	35.96	—	—
$\text{C}_3\text{H}_7\text{NH}_3$	4.98	55.05	—	—
$\text{C}_6\text{H}_{13}\text{NH}_3$	4.98	73.20	—	73.2
$\text{C}_8\text{H}_{17}\text{NH}_3$	4.96	85.05	—	87.0
$\text{C}_{10}\text{H}_{21}\text{NH}_3$	4.96	95.06	—	100.5

characterized by sets of very intense (00L) reflections, though (101) and (110) can also be observed, albeit broadened with respect to  $\text{KNiAsO}_4$ . The calculated lattice parameters are shown in Table II, where they are compared with those obtained by Beneke and Lagaly (1). In contrast, the X-ray powder diffraction profiles of the products from the attempted exchange of  $\text{K}^+$  in  $\text{KNiAsO}_4$  for hydrochlorides of sorbyl, allyl, and propargyl amines showed no signs of layer expansion.

X-ray diffraction profiles of samples of  $\text{KNiAsO}_4$  which had been boiled with dilute acid show that marked structural changes take place as  $\text{K}^+$  is removed. When the  $\text{K}^+$  content is reduced to about half that in  $\text{KNiAsO}_4$  the intense (003) reflection characteristic of the latter remains, but with its *d*-spacing reduced from 9.58 to 8.67 Å, and the (110) reflection arising from the basal plane structure of the parent  $\text{KNiAsO}_4$  can still be seen. After longer reaction periods,

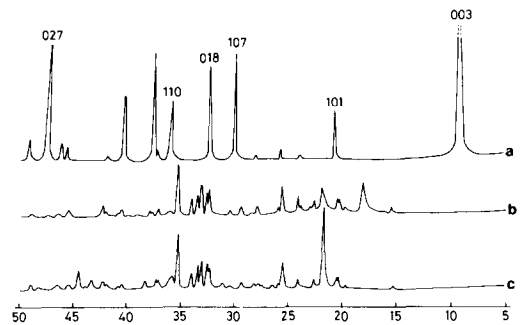


FIG. 2. X-ray powder diffraction profiles of (a)  $\text{KNiAsO}_4$ , (b)  $\text{H}(\text{H}_2\text{O})_x\text{NiAsO}_4$ , and (c) the product from heating (b) in air to 800°C.

however, these reflections progressively disappear and are replaced by peaks of a phase quite different in structure from  $\text{KNiAsO}_4$ .

Figure 2 compares the powder diffraction profiles of  $\text{KNiAsO}_4$ , the hydrated arsenate, and the product of heating the latter at 800°C. The profile of the 800°C product is very similar to that of the hydrated arsenate except in the low-angle region, and both are different from that of  $\text{KNiAsO}_4$ . The X-ray diffraction profile of the 800°C product did not change after exposure to air. High-temperature Guinier photography indicates that structurally there is little change on passing from the hydrated arsenate to the 800°C product. The diffraction pattern of the 800°C product is identified as that of xanthosite,  $\text{Ni}_3(\text{AsO}_4)_2$  (12) (Table III), while the similarity with the room-temperature hydrated arsenate allowed us to assign

TABLE III  
UNIT CELL PARAMETERS FOR X-RAY POWDER DIFFRACTION OF NICKEL ARSENATES

	$a_0$ (Å)	$b_0$ (Å)	$c_0$ (Å)	$\beta$ (°)	No. of reflections		Reference
					fitted		
$\text{Ni}_3(\text{AsO}_4)_2$	10.174	9.548	5.766	92.97	—		(10)
(xanthosite)	10.205(6)	9.580(8)	5.776(5)	92.96(5)	27		This work
$\text{Ni}_3(\text{AsO}_4)_2 \cdot 6\text{H}_2\text{O}$	10.183(8)	9.572(9)	5.765(4)	92.95(7)	25		This work
$\text{Ni}_3(\text{AsO}_4)_2 \cdot 8\text{H}_2\text{O}$ (annabergerite)	10.144	13.241	4.693	104.92	—		(18)

the diffraction pattern of the latter to a similar unit cell.

3.3. Infrared Spectroscopy

In the infrared spectrum of KNiAsO<sub>4</sub> the observed bands due to AsO<sub>4</sub><sup>3-</sup> were assigned as follows:

- $\nu_3$  877 cm<sup>-1</sup> (medium; A)
- 763 cm<sup>-1</sup> (strong; E)
- $\nu_4$  461 cm<sup>-1</sup> (strong; E)
- 421 cm<sup>-1</sup> (medium; A).

The infrared spectra of the propyl- and octylammonium nickel arsenates were compared with those of the solid propyl- and octylammonium chlorides. Table IV shows the bands observed and their assignments. N-H stretching bands are broadened in the IR spectra of compounds containing -NH<sub>3</sub><sup>+</sup> groups. In the present case there is a definite decrease in wavenumber on going from RNH<sub>3</sub>Cl to RNH<sub>3</sub>NiAsO<sub>4</sub>, at least in the case of the asymmetric mode. The symmetric mode cannot be observed, because it is obscured by C-H stretches. On the other hand, the -NH<sub>3</sub><sup>+</sup> deformations are sharp and intense and increase in wavenumber from RNH<sub>3</sub>Cl to RNH<sub>3</sub>NiAsO<sub>4</sub>.

The IR spectrum of the hydrated arsenate is quite different from that of KNiAsO<sub>4</sub>. Both the  $\nu$ (O-H) and  $\delta$ (H<sub>2</sub>O) vibrations disappear together on dehydration and do not appear in the spectrum above 450°C. The number and form of the bands below 1100 cm<sup>-1</sup> remain constant throughout the dehydration. The IR spectra of the 450°C product and final 800°C product are identical.

3.4. Thermal Analysis

The TG and DTA results for KNiAsO<sub>4</sub> and the hydrated arsenate are shown in Fig. 3. No weight loss is observed for KNiAsO<sub>4</sub>, while the hydrated arsenate shows two separate weight losses giving the final product at 600°C. From the DTA curve (Fig. 3a) we estimate the temperatures at which the two distinct weight losses occur and hence the percentage weight losses of each stage from the TG curve as follows:

- first weight loss to 240°C = 9.1%
- second weight loss to ~480°C = 11.03%.

The first weight loss corresponds to a very small endothermic heat change (2 kJ/mole) and the second to a small exothermic heat change. Its unsymmetrical shape sug-

TABLE IV  
INFRARED SPECTRA OF K<sub>x</sub>(RNH<sub>3</sub>)<sub>(1-x)</sub>NiAsO<sub>4</sub> AND RCl (R = C<sub>3</sub>H<sub>7</sub>NH<sub>3</sub>, C<sub>8</sub>H<sub>17</sub>NH<sub>3</sub>)

Assignment	C <sub>3</sub> H <sub>7</sub> NH <sub>3</sub> Cl	C <sub>3</sub> H <sub>7</sub> NH <sub>3</sub> NiAsO <sub>4</sub>	C <sub>8</sub> H <sub>17</sub> NH <sub>3</sub> Cl	C <sub>8</sub> H <sub>17</sub> NH <sub>3</sub> NiAsO <sub>4</sub>	KNiAsO <sub>4</sub>
N-H stretch (as)	3200 m <sup>a</sup>	3160 st/b	3200 m	3170 st/b	
N-H stretch (s)	3010 st	*	3010 st	*	
NH <sub>3</sub> <sup>+</sup> def. (as)	1595 st	1637 m	1590 st	1640 m	
NH <sub>3</sub> <sup>+</sup> def. (s)	1525 st	1535 m	1525 st	1540 m	
AsO <sub>4</sub> ( $\nu_3$ )A		850 st		860 st	877 st
		770 st		775 st	763 st
AsO <sub>4</sub> ( $\nu_4$ )E		465 st		463 st	461 st
AsO <sub>4</sub> ( $\nu_4$ )A		430 st		430 st	421 st

<sup>a</sup> as = Asymmetric, s = symmetric, def = deformation, st = strong, m = medium, b = broad, \* = obscured by C-H stretches.

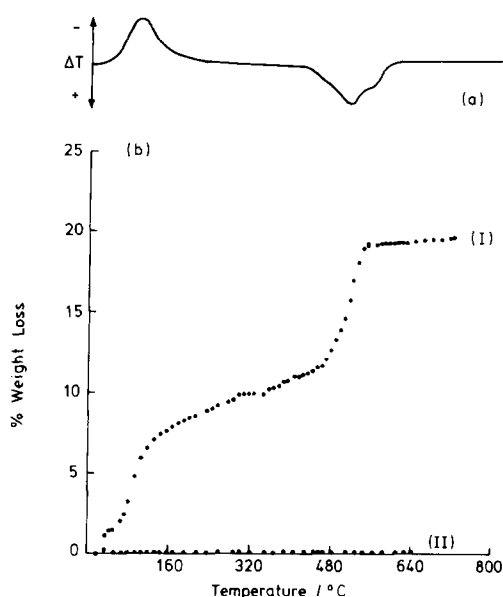


FIG. 3. (a) Differential thermal analysis of  $\text{H}(\text{H}_2\text{O})_x\text{NiAsO}_4$  and (b) thermogravimetric analysis of (I)  $\text{H}(\text{H}_2\text{O})_x\text{NiAsO}_4$  and (II)  $\text{KNiAsO}_4$ .

gests that two heat changes are superimposed.

### 3.5. Magnetic Susceptibility

Magnetic susceptibility measurements were made on samples of  $\text{KNiAsO}_4$  and

$\text{C}_{10}\text{H}_{21}\text{NH}_3\text{NiAsO}_4$ . Figure 4 shows the variation of  $\chi$  with temperature for each compound. The Neel temperatures,  $T_N$ , may be estimated from the inflections on the low-temperature side of the broad maxima. For  $\text{KNiAsO}_4$  and  $\text{C}_{10}\text{H}_{21}\text{NH}_3\text{NiAsO}_4$  they are 15.9(1) and 19.3(2) K, respectively. The temperatures  $T(\chi_{\max})$ , where  $\chi$  is a maximum, are  $25.0 \pm 0.5$  and  $25.7 \pm 0.5$  K, respectively.

### 3.6. Optical Measurements

The room-temperature electronic spectrum of a crystal of  $\text{KNiAsO}_4$  in the visible region contains three bands, assigned as transitions of octahedral Ni(II) as follows:

$$\begin{aligned} 23,800 \text{ cm}^{-1}: & \ ^3T_{1g}(P) \leftarrow ^3A_{2g}(F) \\ 22,880 \text{ cm}^{-1}: & \ ^1T_{2g}(D) \leftarrow ^3A_{2g}(F) \\ 13,700 \text{ cm}^{-1}: & \ ^3T_{1g}(F) \leftarrow ^3A_{2g}(F). \end{aligned}$$

These agree with the spectrum of Ladwig and Ziemer (4), who also observed the  $^3T_{2g}(F) \leftarrow ^3A_{2g}(F)$  band at  $8400 \text{ cm}^{-1}$ . The 15 K spectrum is shown in Fig. 5. At this temperature the  $13,700\text{-cm}^{-1}$  band becomes doubled with a well-resolved vibronic progression on the high-wavenumber side, which originates from a sharp band at

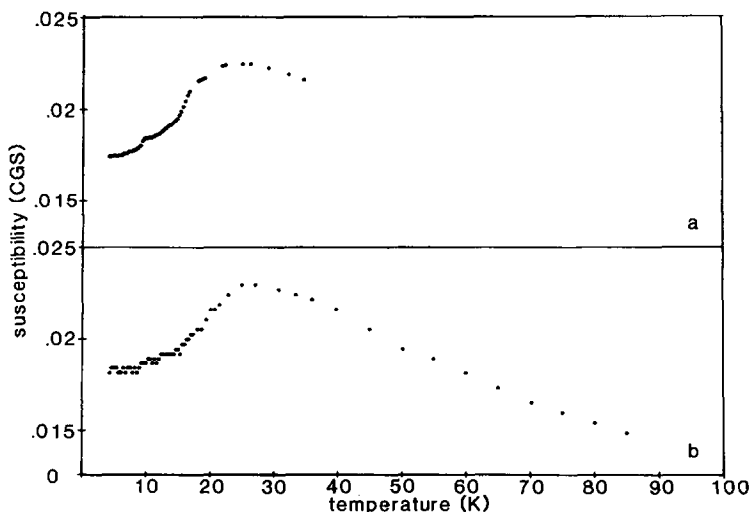


FIG. 4. Magnetic susceptibility versus temperature for (a)  $\text{KNiAsO}_4$  and (b)  $(\text{C}_{10}\text{H}_{21}\text{NH}_3)\text{NiAsO}_4$ .

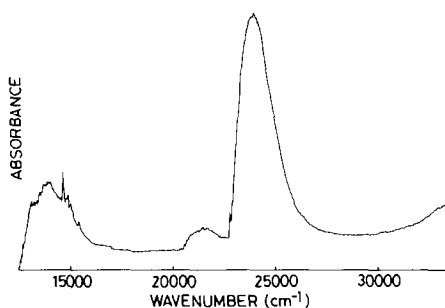


FIG. 5. Single-crystal transmission spectra of KNiAsO<sub>4</sub> at 15 K.

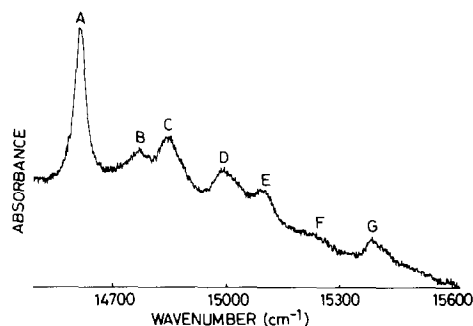


FIG. 6. Fine structure of the 15,000-cm<sup>-1</sup> band in KNiAsO<sub>4</sub> at 15 K.

14,628 cm<sup>-1</sup> (Fig. 6). The wavenumbers of the peaks in this region and the intervals between them are given in Table V.

On the low-wavenumber side of the 23,800-cm<sup>-1</sup> band a sharp band appears at 22,692 cm<sup>-1</sup>, whose temperature dependence is shown in Fig. 7. With increasing temperature it diminishes in height and broadens. We observed no field effects in the absorption spectrum of this band between  $B = 0$  and  $B = 5T$  applied either parallel or perpendicular to the planes.

#### 4. Discussion

##### 4.1. Substitution of Organic Cations in KNiAsO<sub>4</sub>

The chemical analyses and X-ray powder diffraction profiles show the ion exchange

of K<sup>+</sup> in KNiAsO<sub>4</sub> with C<sub>n</sub>H<sub>2n+1</sub>NH<sub>3</sub><sup>+</sup> takes place quite readily especially where  $n > 5$ . In contrast, under comparable conditions very little exchange of RNH<sub>3</sub><sup>+</sup> occurs when  $R$  contains a double or triple bond. The failure of the ion exchange in these cases may be due to the rigidity of the chain containing an unsaturated link which prevents it from orientating into a favorable position between the layers. The C<sub>n</sub>H<sub>2n+1</sub>NH<sub>3</sub><sup>+</sup> chains are flexible and may twist themselves into the lowest energy packing arrangement.

The interlayer spacings of the alkylammonium derivatives (Table II) agree with those obtained by Beneke and Lagaly (1) and extend their results to shorter chain lengths. The regular increase in the interlayer spacing with alkyl chain length is observed in many inorganic-organic systems

TABLE V  
VIBRONIC FINE STRUCTURE IN THE 4.2 K ABSORPTION SPECTRUM OF KNiAsO<sub>4</sub>

Peak (cm <sup>-1</sup> )	Difference (cm <sup>-1</sup> )	Difference (cm <sup>-1</sup> )	Difference (cm <sup>-1</sup> )
<i>a</i> 14,628	<i>a</i> → <i>c</i> 232	<i>a</i> → <i>d</i> 375	<i>b</i> → <i>f</i> 456
<i>b</i> 14,784	<i>c</i> → <i>e</i> 245	<i>d</i> → <i>g</i> 395	
<i>c</i> 14,859			
<i>d</i> 15,002			
<i>e</i> 15,104			
<i>f</i> 15,240			
<i>g</i> 15,390			

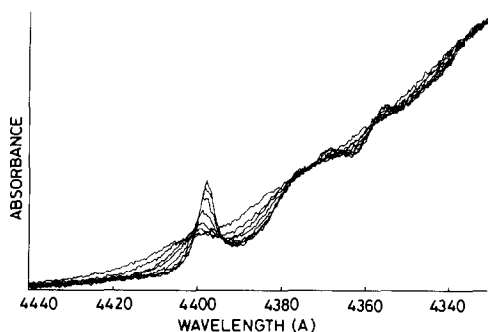


FIG. 7. The  $22,700\text{-cm}^{-1}$  band in  $\text{KNiAsO}_4$  at different temperatures between 5 and 40 K.

(11) and is indicative of a highly ordered interlayer structure. The mean increase of the interlayer spacings with a number of carbon atoms indicates that the chains are arranged in bilayers tilted at  $60\text{--}65^\circ$  to the basal plane. Angles of tilt for similarly charged clays are usually between  $50$  and  $65^\circ$  to the basal plane, the angle being determined by hydrogen bonding of the  $\text{RNH}_3^+$  to the oxygen atoms of the inorganic layer. Such hydrogen bonding is observed in kaolinite-hydrazine (12) and high layer charge montmorillonites and vermiculites (13). In these clay minerals the hydrogen atoms of the  $-\text{NH}_3^+$  groups may be bonded to one, two, or three silicate oxygen atoms depending on the angle of tilt and the unit cell parameters (14, 15).

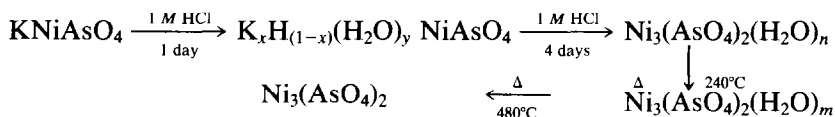
Hydrogen bonding causes a decrease in the frequency of the  $X\text{--H}$  stretching vibration ( $X = \text{O}$  or  $\text{N}$ ) as found for the asymmetric  $\text{N--H}$  stretch in Table III. Similarly the frequency of the  $-\text{NH}_3^+$  deformation is expected to increase because of the restriction in motion (16). In fact the  $-\text{NH}_3^+$  deformation bands of the  $\text{RNH}_3\text{NiAsO}_4$  are

strong and sharp, and appear  $50\text{ cm}^{-1}$  higher than in  $\text{RNH}_3\text{Cl}$  (Table IV).

We cannot say definitely how many hydrogens are bonded to which oxygen atoms in  $\text{RNH}_3\text{NiAsO}_4$ . However, Brindley (15) found that for alkylammonium montmorillonites having an angle of tilt  $65^\circ$  and  $a_0$  parameter  $5.18\text{ \AA}$ , the geometry favored hydrogen bonding between two  $-\text{NH}_3^+$  hydrogens and pairs of silicate oxygens. Since the  $\text{RNH}_3\text{NiAsO}_4$  compounds have similar geometry (angle of tilt  $60\text{--}65^\circ$  and  $a_0$  parameter  $4.99\text{ \AA}$ ) they may exhibit similar hydrogen bonding.

#### 4.2. Hydrated Derivatives of $\text{KNiAsO}_4$

The product of reacting  $\text{KNiAsO}_4$  with dilute acid for 4 days no longer contains any  $\text{K}^+$ , though the infrared spectrum shows that it contains  $\text{H}_2\text{O}$ . As has been found previously for other  $\text{Ni(II)}$  arsenates (17), full elemental analysis of the product is made difficult by its insolubility, but the  $\text{Ni}:\text{As}$  ratio is  $3:2$  rather than  $1:1$ . The phase obtained by heating the hydrated  $\text{Ni(II)}$  arsenate to  $800^\circ\text{C}$  is readily identified as xanthosite,  $\text{Ni}_3(\text{AsO}_4)_2$  (10), so the great similarity between the X-ray diffraction profiles of the room-temperature and  $800^\circ\text{C}$  products suggests very strongly that the former is a hydrated form of xanthosite containing a similar cation-anion lattice. It was noted in Section 3.2 that if  $\text{K}^+$  is only partly removed from  $\text{KNiAsO}_4$ , by reacting it with dilute acid for 1 day, the X-ray profile remains similar to that of  $\text{KNiAsO}_4$ , albeit with a reduction in interlayer spacing. We therefore put forward the following reaction scheme:



The weight losses observed by TGA give values of  $n$  and  $m$  of 5.95 and 3.12, respec-

tively. It is interesting that hydrated  $\text{Ni(II)}$  *ortho*-arsenate formed by reacting  $\text{KNi-}$

AsO<sub>4</sub> with acid is different to annabergerite (18), the naturally occurring Ni<sub>3</sub>(AsO<sub>4</sub>)<sub>2</sub> · 8H<sub>2</sub>O.

The dehydration scheme indicates the presence of H<sub>2</sub>O in the lattice up to the temperature of the second weight loss, at 480°C. In the case of compounds containing only interlayer water it is somewhat unusual for water to remain at such a high temperature. For example, interlayer water in MoO<sub>3</sub> · 2H<sub>2</sub>O and WO<sub>3</sub> · 2H<sub>2</sub>O is expelled at 50 and 100°C, respectively (19, 20). On the other hand, in the β-alumina hydrates, dehydration to α-Al<sub>2</sub>O<sub>3</sub> does not occur until 700°C (21, 22). Complete dehydration of clays usually occurs between 400 and 600°C (23), and the final stage is dehydroxylation—loss of -OH as H<sub>2</sub>O from M-OH units (M = Al or Mg).

The variable-temperature Guinier-Simon photograph of hydrated nickel arsenate revealed a gradual evolution of the diffraction pattern parameters with no abrupt changes. Thus hydrated nickel *ortho*-arsenate and xanthosite are isomorphs with almost identical lattice parameters. This suggests that the whole dehydration is topotactic. The IR bands below 1100 cm<sup>-1</sup> due to metal-oxygen stretching and bending vibrations are present throughout the dehydration process.

#### 4.3. Magnetic Measurements

The plots of  $\chi$  versus  $T$  for KNiAsO<sub>4</sub> and C<sub>10</sub>H<sub>21</sub>NH<sub>3</sub>NiAsO<sub>4</sub> display the broad maxima characteristic of low-dimensional magnetic systems. The similarity in the behavior of the two compounds, despite a difference in interlayer spacing of ~27 Å, suggests that KNiAsO<sub>4</sub> is already a good approximation to a low-dimensional antiferromagnet.

Our data are not sufficiently accurate to fit to a series expansion, but it is valid to extract values of the exchange constants  $J$  from the values of  $T(\chi_{\max})$  since in general

the latter have been shown to be proportional to  $JS(S + 1)$ , where  $S$  is the spin (26). From Rushbrooke and Wood's series expansion for an  $S = 1$  honeycomb lattice Heisenberg antiferromagnet (26), we find that  $T(\chi_{\max}) \approx 1.67 (J/k) S(S + 1)$ , which gives  $J \approx -7.5(1)$  K for KNiAsO<sub>4</sub> and  $-7.7(1)$  K for C<sub>10</sub>H<sub>21</sub>NH<sub>3</sub>AsO<sub>4</sub>. Thus the near-neighbor intralayer exchange constants are almost identical. It is also interesting to note that, at least in the case of KNiAsO<sub>4</sub>,  $T_N \approx (J/k)(S + 1)$  in accord with predictions for two-dimensional antiferromagnets (7).

Neutron scattering and specific heat experiments by Regnault *et al.* (6) have established that BaNi<sub>2</sub>(AsO<sub>4</sub>)<sub>2</sub>, which has a structure similar to that of KNiAsO<sub>4</sub> but a slightly smaller interlayer spacing (7.87 Å compared with 9.58 Å), behaves as a two-dimensional XY antiferromagnet with  $T_N = 19$  K.

Susceptibility and neutron scattering experiments are in progress to further characterize the magnetic behavior of this series of compounds.

#### 4.4. Optical Measurements

At room temperature, the visible and near-infrared transmission spectra of a crystal of KNiAsO<sub>4</sub> contain two spin-allowed ligand field transitions ( ${}^3T_{1g}(F) \leftarrow {}^3A_{2g}(F)$ , 13,700 cm<sup>-1</sup>, and  ${}^3T_{1g}(P) \leftarrow {}^3A_{2g}(F)$ , 23,800 cm<sup>-1</sup>) and a weak spin-forbidden transition ( ${}^1T_{2g}(D) \leftarrow {}^3A_{2g}(F)$ ) in agreement with the powder diffuse reflectance spectrum of Ladwig and Zeimer (4).

From the energies of the two spin-allowed transitions we calculate that  $B = 856$  cm<sup>-1</sup> and  $10D_q = 8390$  cm<sup>-1</sup>. (The value of  $B$  for the free Ni<sup>2+</sup> ion is 1040 cm<sup>-1</sup>.) At low temperature the band centered around 13,700 cm<sup>-1</sup> splits and a vibrational progression appears to the high-wavenumber side (Fig. 6). Solomon and Ballhausen studied the structure of this so-called "red"

band for  $\text{Ni}(\text{H}_2\text{O})_6^{2+}$  in various lattices with a decreasing site symmetry at the  $\text{Ni}^{2+}$  ion (24). Fine structure observed on the high-wavenumber side of the band originated from two sharp origins. It was found that, except for the  $O_h$  site symmetry case, the origins were split. For octahedrally coordinated  $\text{Ni}^{2+}$ , crystal-field theory predicts an  ${}^1E_g$  state almost degenerate with  ${}^3T_{1g}(F)$ . The  ${}^1E_g$  has double group symmetry  $\Gamma_{3g}$  and is capable of being mixed by the spin-orbit interaction with a  $\Gamma_{3g}$  component derived from  ${}^3T_{1g}$ .

A similar situation arises in  $\text{KNiAsO}_4$ . The fine structure observed at low temperatures is probably caused by the  ${}^1E_g(D) \leftarrow {}^3A_{2g}(F)$  transition, allowed by the spin-orbit mechanism. On the other hand, the sharp origin is not split, suggesting, by analogy with Solomon and Ballhausen (24), that the  $O_h$  field at the  $\text{Ni}^{2+}$  is not distorted. The vibrational intervals ( $\sim 240$ , 385, and tentatively  $450\text{ cm}^{-1}$ ) built on the  ${}^1E_g$  origin cannot be assigned to specific Ni-O modes without a complete assignment of the far IR and Raman spectra of  $\text{KNiAsO}_4$ .

Figure 5 shows that in addition to the  ${}^1T_{2g}(D) \leftarrow {}^3A_{2g}(F)$  band between  $21,000$  and  $22,000\text{ cm}^{-1}$  there is a further sharp weak band at  $22,692\text{ cm}^{-1}$ , at the foot of the intense  ${}^3T_{1g}(P) \leftarrow {}^3A_{2g}(F)$  absorption. The temperature variation of this band is given in Fig. 7, from which one can see that with increasing temperature it broadens rapidly and shifts to lower frequency. Other ill-defined structures between  $22,750$  and  $23,000\text{ cm}^{-1}$  appear to arise from vibronic sidebands built on the  $22,692\text{-cm}^{-1}$  origin. Though the  $22,692\text{-cm}^{-1}$  band has broadened at 40 K so much that it has almost vanished into the baseline, its area does not vary significantly, nor is it magnetic field dependent. Thus we assign it as the electronic origin line of the  ${}^3T_{1g}(P) \leftarrow {}^3A_{2g}(F)$  transition rather than another spin-forbidden transition such as  ${}^1A_{1g}(G) \leftarrow {}^3A_{2g}(F)$ .

## 5. Conclusions

Alkylammonium ions  $\text{C}_n\text{H}_{2n+1}\text{NH}_3^+$  exchange quite readily with  $\text{K}^+$  in the synthetic mica analogue  $\text{KNiAsO}_4$ . However, under the same conditions alkylammonium ions containing unsaturated bonds exchange to a far more limited extent.

Warming  $\text{KNiAsO}_4$  with dilute acid for several hours leads to the partial exchange of  $\text{K}^+$  by  $\text{H}_3\text{O}^+$ , with a slight decrease in interlayer spacing. Prolonged reaction with acid leads to the formation of  $\text{Ni}_3(\text{AsO}_4)_2 \cdot 6\text{H}_2\text{O}$ , a new hydrated form of xanthiosite,  $\text{Ni}_3(\text{AsO}_4)_2$ . The dehydration of  $\text{Ni}_3(\text{AsO}_4)_2 \cdot 6\text{H}_2\text{O}$  to give xanthiosite is topotactic.

Both  $\text{KNiAsO}_4$  and  $\text{C}_{10}\text{H}_{21}\text{NH}_3\text{NiAsO}_4$  are new examples of a two-dimensional antiferromagnet with a honeycomb lattice and order at 15.9(1) and 19.3(2) K, respectively.

## Acknowledgments

This work was supported in part by the UK Science and Engineering Research Council. We thank Mr. F. Wondre, Dr. J.R.G. Thorne, and Dr. S. Crouch-Baker for technical assistance.

## References

1. K. BENEKE AND G. LAGALY, *Clay Miner.* **17**, 175-183 (1982).
2. C. LEFEVRE, *C.R. Acad. Sci. Paris* **110**, 405 (1890).
3. C. LEFEVRE, *Ann. Chim. Phys.* **27**, 1-62 (1892).
4. G. LADWIG AND B. ZIEMER, *Z. Anorg. Allg. Chem.* **457**, 143-148 (1979).
5. K. J. RANGE AND H. MEISTER, *Z. Naturforsch., B. Anorg. Chem., Org. Chem.* **39**, 118-120 (1984).
6. L. REGNAULT, J. HENRY, J. ROSSAT-MIGNOD, AND A. DE COMBARIEU, *J. Magn. Magn. Mater.* **15-18**, 1021-1022 (1980).
7. L. DE JONGH AND A. MIEDEMA, *Adv. in Phys.* **23**, 1 (1974).
8. B. TIEKE AND G. WEGNER, *Makromol. Chem. Rapid. Commun.* **2**, 543-549 (1981).
9. G. LAGALY, M. FERNANDEZ-GONZALEZ, AND A. WEISS, *Clay Miner.* **11**, 173 (1976).

10. R. J. DAVIS, M. H. HEY, AND A. W. G. KINGSBURY, *Mineral. Mag.* **35**, 72 (1964).
11. A. WEISS, *10th Nat. Conf. Clay Miner.* **12**, 191–224 (1963).
12. T. LEDOUX AND J. WHITE, in "Proceedings, 1st International Clay Conference' Jerusalem, 1966," pp. 361–374.
13. G. LAGALY, *Clays. Clay Miner.* **30**(3), 215–222 (1982).
14. G. LAGALY, *Adv. Coll. Int. Sci.* **11**, 105–148 (1979).
15. G. W. BRINDLEY, *Clay Miner.* **6**, 91 (1965).
16. K. NAKAMOTO, "Infrared Spectra of Inorganic and Coordination Compunds," Wiley, New York (1978).
17. T. ISAACS, *Mineral. Mag.* **33**, 663 (1963).
18. "Dana's System of Mineralogy," 7th ed., Vol. 2, p. 747.
19. O. GLEMSE AND G. LUTZ, *Z. Anorg. Allg. Chem.* **264**, 17 (1951).
20. M. S. WHITTINGHAM AND A. J. JACOBSON (EDS), "Intercalation Chemistry," Academic Press New York (1982).
21. G. FARRINGTON, W. ROTH, AND M. BREITER, *J. Solid State Chem.* **24**, 321–330 (1978).
22. G. FARRINGTON, M. BREITER, W. ROTH, AND J. DUFFY, *Mater. Res. Bull.* **12**, 895 (1977).
23. DEER, HOWIE, AND ZUSSMAN (EDS.), "Introduction to the Rock Forming Minerals, Longmans, Green, NY (1966).
24. E. SOLOMON AND C. J. BALLHAUSEN, *Mol. Phys.* **29**, 279–299 (1975).
25. A. M. BUCKLEY, Part II Thesis, Oxford University, Oxford (1985).
26. G. S. RUSHBROOKE AND P. J. WOOD, *Mol. Phys.* **1**, 257 (1958).